

# Use of Electrochemical Impedance Spectroscopy (EIS) for the Evaluation of Electrocoatings Performances

Marie-Georges Olivier<sup>1</sup> and Mireille Poelman<sup>2</sup>

<sup>1</sup>University of Mons, Materials Science Department, Mons,

<sup>2</sup>Materia Nova Research Centre, Mons,  
Belgium

## 1. Introduction

Thanks to their barrier properties against corrosive species, organic coatings are often used to protect metals against corrosion. In the automotive industry, cathodic electrocoating is widely used as a primary layer coating in the corrosion protection system [1-3]. This deposition method has many advantages including high throw power, high corrosion protection and coating transfer coefficient (>95%), auto-limitation of the coating thickness, environmentally friendly due to an aqueous suspension medium and an easy industrial automation [4, 5]. This coating can also be applied on each metal composing the car body.

Corrosion protection is guaranteed only if good adhesion properties are attained between the metallic substrates and the coating. Enhanced adhesion can be achieved by the use of an appropriate surface preparation prior to coating (etching, polishing, etc.) or with a good pre-treatment which can also provide additional corrosion protection and adherence [6-9]. So an appropriate combination of surface preparation, pretreatment and coating provides increased durability of the protective system.

As high durability systems are continuously developed, short-term test methods are required to evaluate the corrosion resistance of paint/metal systems and decide among coatings designed for long-term durability. The principle of usual ageing tests is based on the application of specific stresses (temperature, humidity, salts, UV light) at higher levels than in natural exposure to induce accelerated deterioration of the system. A first objective of an accelerated test is to cause the degradation of the coating or its failure in a shorter time period than under natural conditions without changing the failure mechanisms. So far a direct correlation between natural degradation and the weathering device currently being used is not clear, therefore accelerated tests are generally only used for comparative purposes. The degradation of the coating can be obtained using different ageing tests such as immersion in electrolyte, continuous salt fog or SO<sub>2</sub> exposure. Cyclic corrosion tests combining different kinds of exposures (humidity, salt fog, drying steps) are also increasingly used [10-14]. These methods are based on the principle that corrosion can only occur if electrolyte and oxidant species are present at the metal surface. The increase of temperature allows accelerating the transport of oxygen and electrolyte through paint and

initiating the corrosion reactions. For some accelerated tests, use is made of scratched panels to simulate coating damage and delamination. This type of acceleration is essentially related to the damage of protective properties of the coating/pre-treatment/metal system and not to the barrier properties of the coating. As the protective properties of electrocoating systems are continuously improved ageing tests necessitate increasing times before any visual observation of the initiation of degradation is possible.

Electrochemical Impedance Spectroscopy is a powerful tool which was widely used in the last decades to characterize corrosion processes as well as protective performances of pre-treatments and organic coatings [15-28]. This electrochemical technique is not destructive and can consequently be used to follow the evolution of a coated system exposed to an accelerated ageing test and provide, in short time, information about the corrosion kinetics.

In the automotive industries, the most challenging failure modes needing to be detected and evaluated are: the barrier properties of the electrocoating during immersion, thermal cycles or salt spray test; the behavior of a scratched sample in terms of extension of the delaminated area for different kinds of exposures and the specific corrosion at the edges.

The aim of this chapter is to describe the cataphoretic electrodeposition process and to demonstrate by some practical examples that Electrochemical Impedance Spectroscopy can be a very useful tool to provide a complete evaluation of the corrosion protection properties of electrocoatings.

## **2. Cataphoretic electrocoating**

The electrodeposition process was used for the first time in 1963 by Ford in USA to paint spare parts. The process was based on the anodic electrodeposition. In 1967, PEUGEOT was the first car manufacturer to employ this process to coat the whole body car by anaphoresis. In 1978, Chrysler-France in Poissy was the first European line to coat body cars by using cationic paint. Since then, all the manufacturers protect vehicles against corrosion by cataphoresis [1].

In cationic coatings, positively charged coating particles dispersed in an aqueous solution are electrophoretically attracted to a substrate, which is the cathode of the electrolytical cell. The increase of pH due to water reduction at the cathode induces the electrocoagulation of the coating on the substrate. In the case of anaphoresis, the substrate is the anode and the coating binder is charged negatively. In both processes, thermosetting binders are used. In this chapter, only the cataphoresis process will be described.

Cationic electrodeposition presents numerous advantages: self-limitation of the coating thickness, low water permeability (dense network), good adherence and adhesion, high throw power, automation ability, low loss in products, low pollution level and high corrosion protection.

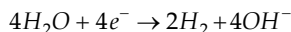
### **2.1 Principle**

In cataphoresis, the metallic substrate is linked to the negative terminal of an electrochemical cell and immersed in the coating bath during more or less two minutes. Under the effect of the electrical field induced by application of a high voltage difference (in

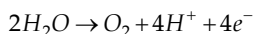
the range of 200 V to 500 V) between the piece (cathode) and the counter-electrode in a low conductivity paint bath, the positively charged coating particles (grafting of amine groups), move towards the cathode by electrophoresis.

The electrochemical reactions are the following:

- **At the cathode (piece to coat):** water electrolysis with hydrogen production and OH<sup>-</sup> formation. This reaction provokes a local increase of pH which neutralizes the NH<sub>3</sub><sup>+</sup> groups fixed on the binder. The particle becomes insoluble in water and settles on the metallic substrate. This step corresponds to the electrocoagulation of the paint.



- **At the anode (counter-electrode):** water is electrolyzed with oxygen evolution and H<sup>+</sup> production. This increase of H<sup>+</sup> ions raises the bath conductivity.



At last, the water contained in the coating layer is expelled by electro-osmosis (water movement under the action of electrical field through the porous layer).

In brief, the coating cathodic electrodeposition is the result of four elementary phenomena (Figure 1):

1. Electrophoresis;
2. Water electrolysis;
3. Coating electrocoagulation;
4. Water electro-osmosis.

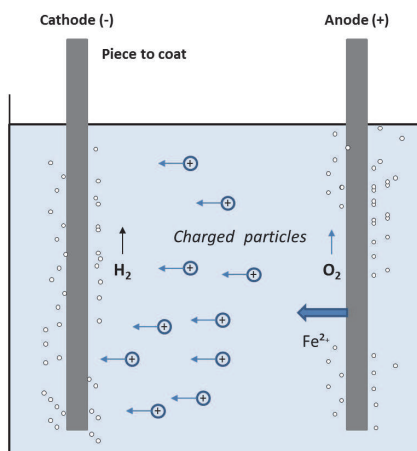


Fig. 1. Schematic representation of cathodic deposition.

The resins used in the formulation of cationic automotive primers (E-coat) are based on epoxy resins. The epoxy resin is reacted with an aminoalcohol, such as diethanolamine (DEA) to obtain a resin with amine and hydroxyl groups. The resin product reacts with an isocyanate half-blocked with an alcohol as 2-ethylhexylalcohol or 2-butoxyethanol for

example in order to make a self cross-linkable resin [29]. Catalyst and pigment dispersions (titane dioxide or carbon black) are added. In aqueous medium the pigments have a charge which is insufficient to form a homogeneous suspension. The ionized binder surrounds them as a protective colloid and insures suspension homogeneity and stability. The pigment diameter must be lower than one micron.

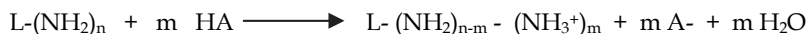
The amine groups are neutralized with a volatile carboxylic acid such as acetic or formic acids before dispersion in water. The neutralization rate plays an important role in the stability and deposit process of the coating. In order to determine this parameter, a titration of a known amount of paint by HCl and KOH allows calculating the numbers of alkaline (Basic Meq) and acid (Acid Meq) milliequivalents, respectively.

The neutralization rate is given by equation (3):

$$T_n = \frac{\text{Alkaline Meq}}{\text{Acid Meq} + \text{Alkaline Meq}}$$

It is usually in the order of 40-50%.

The binder is insoluble in water but can be dispersed thanks to the ionization of fixed groups. This ionization is carried out by using an acid according to the following reaction step:



The electrocoagulation step is the opposite of the solubilization operation. The neutralized form of the binder being insoluble in water and hydrophobic, the disposal of liquid paint can be done by water rinsing. This property is employed to recover and recycle the paint excess. The water is also expelled during the electro-osmosis step. This phenomenon allows diminishing the energy consumption during the curing. The water weight percent in the layer is around 10-15% before baking.

After electrocoagulation, the film has to be reticulated by curing at controlled temperature. This operation confers the definitive properties to the film: adherence, hardness, corrosion resistance. During this step, the blocked isocyanate reacts with a hydroxyl group of the epoxy resin to form a urethane cross-link. Older E-coat primers contained basic lead silicate as a catalyst, which interacted with the phosphate layer to enhance adhesion. Lead-free E-coats have replaced the older formulations [30, 31].

## 2.2 Industrial process

The installations (Figure 2) are preceded by a surface treatment area (phosphating or alternative pretreatments) and followed by a curing area (around 30 min at 130-180°C).

The industrial process is composed of the following steps:

- Coating bath ;
- Systems to maintain bath stability ;
- Rinsing installation ;
- Power supply ;
- Conveyer.

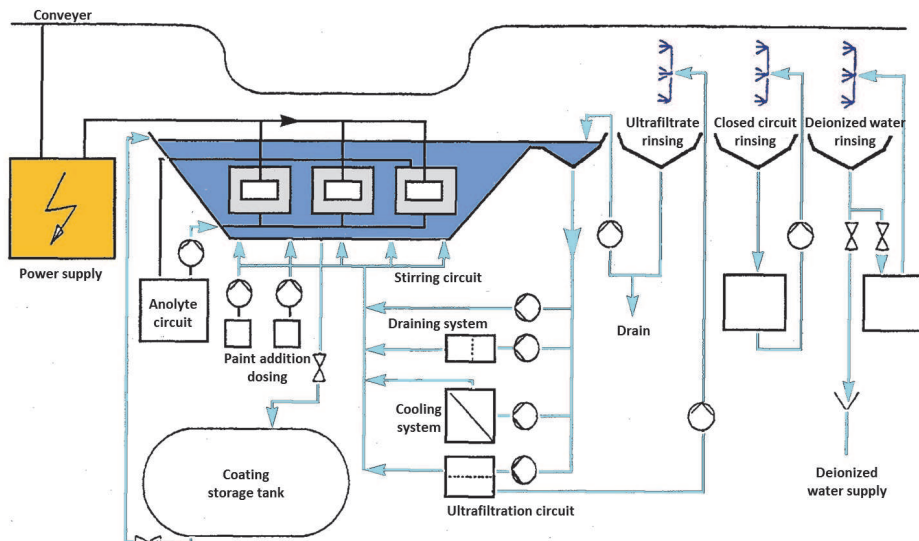


Fig. 2. Schematic representation of industrial process of cathoporesis.

### Bath coating

The capacity and the bath dimensions are depending on the size of the pieces to coat. The tank is in PVC or in steel covered by corrosion protection coating. An overflow, built on the side of the tank, supplies the different circuits.

### Fluids circulation

- **Coating circulation:** the stirring of the coating is carried out by an external coating circuit supplied by a pump. In order to have a sufficient stirring, the pumped coating must be reintroduced by injection nozzles located in the bottom or on the lateral faces of the tank. This circulation prevents the coating flocculation.
- **Filtration circuit of the paint:** Elimination of the impurities carried into the bath is achieved by continuous filtration.
- **Cooling system:** the quality of the coating can only be insured and reached in a narrow range of temperature. The heating of the bath is due to the current flow, bath stirring or due to the heat brought by the pieces coming from the surface treatment.
- **Ultrafiltration circuit:** Despite the fact that the film thickness is controlled by the applied voltage, there is always during emersion a supplementary entrainment of paint which has to be eliminated by rinsing. The paint contained in rinsing water can be recovered and recycled by ultrafiltration. This technique consists in a separation on a membrane. The matters flow through the membrane is achieved by pressure application depending on the average size of the membrane pores. The ultrafiltration membranes have an average porosity comprised between 0.001 and 0.1  $\mu\text{m}$  and work under pressure from 1 to 10 bar. The retained matters, also called concentrates, are binder macromolecules, pigments and fillers. The matters which cross the membrane are the ultrafiltrate composed of dissolved compounds. The dry content is around 1%. The ultrafiltrate is used in the rinsing system. The concentrate is recycled towards the coating bath.

- **Draining circuit of impurities:** The bath is contaminated by impurities coming from surface treatments and altering the paint. These impurities, non-stopped by membrane, are continuously eliminated thanks to a draining system located in the ultrafiltration circuit. This draining is compensated by addition of deionized water. Depending on the quality and the nature of rinsing after surface treatment, order of 0.001 to 0.005 liter of ultrafiltrate per painted square meter is rejected.
- **Anolyte circuit:** The acid needed for binder neutralization (produced at the anode) is not eliminated after electrocoating and enriches the bath. Being harmful the acid excess is extracted by electrodialysis on cationic membrane. This method consists of protons transport through a selective membrane under the effect of an electrical voltage and their concentration in an anodic compartment of the electrodialysis cell where they are extracted and replaced by deionized water. This circuit allows maintaining the bath pH at 6-7.
- **Circuit of paint addition:** the paint deposited on the pieces must be compensated by addition of a preparation concentrated in binder, pigments and fillers. These compounds are either premixed outside the tank with the bath paint or directly introduced from the stirring circuit.

#### *Rinsing system*

During emersion of the pieces, non-coagulated paint is carried by capillarity and retention in the pores. This paint amount can reach from 25% to 45% of the consumed paint and must be removed by rinsing before curing due to its different characteristics. The pieces rinsing is done in three steps. During the first step, the film is rinsed with ultrafiltrate. For the second rinsing, a closed circuit is used. For the high quality coatings, a third rinsing is performed with deionized water. Before curing, the pieces are dried by air flushing.

#### *Power supply*

The electrocoating installations require a power supply in continuous current with voltage in the range of 200 – 400 V (1 to 10 mA/cm<sup>2</sup>).

#### *Conveyer*

Conveyer allows the pieces transport but also constitutes the negative terminal of the generator. The conveyer design must take into account the immersion duration, positioning and number of pieces to coat.

### **2.3 Advantages, drawbacks and challenges**

#### *Effect of application parameters*

The main parameters needing control during electrodeposition are voltage, bath conductivity and temperature [32].

The rate of deposition is strongly affected by applied voltage: the higher voltage induces a faster deposition. The conveyer is designed to obtain a coating in 2 to 3 min at a voltage comprised between 225 and 400 V. The high voltage increases the driving force for electrophoretic attraction of the particles to the cathode and allows an adequate covering of the confined areas. The first areas covered are the edges of the metallic substrate due to their highest current density. The electrical resistance rises with the film thickness reducing the

rate of electrodeposition. There is a limiting film thickness beyond which the coating deposition stops or at least becomes very slow. When the edges are coated, outer flat surfaces of the body car are coated, followed by recessed and confined areas. For corrosion protection, it is needed to have the entire surface of the metal coated and to coat the furthest confined areas within the 2 to 3 minutes dwell time in the tank. The deposition in the recessed area explains the high throw power of electrocoating which increases with the applied voltage and the duration in the bath. However, if the applied voltage is too high, a film rupture on the outer surfaces will be observed due to current flow leading to local generation of hydrogen under the film. The generation of gas bubbles blowing out through the film induces film defects. Throw power is also affected by the bath conductivity: a higher conductivity induces a greater throw power. Nevertheless, there is a limitation, an increase of bath conductivity modifies the conductivity of the film (presence of soluble salts) induces an increase of the ionic strength and so a loss of the bath stability due to decrease of the zeta potential of the double layer capacitance at the interface between the charged particles and the bath. A compromise must consequently be reached. The bath conductivity is from 1200 to 1800  $\mu\text{S}/\text{cm}$ .

The properties of the film are also strongly depending on the temperature which must be controlled in a very narrow range, typically 32 to 35°C.

#### *Advantages and drawbacks*

Electrodeposition is a highly automated system and requires only one operator. The transfer coefficient is higher than 95%. However, the financial investment of the automated line is high, limiting applicability of these lines to large production processes. The electrodeposition unit is the most expensive equipment in an auto assembly plant.

Solvent content of E-coats is relatively low, so VOC emissions are limited and fire risk reduced. The complete coverage of surfaces is another advantage. Even if differences are observed in film thicknesses, the inner areas having thinner layer than the exposed face areas, the entire surface will be protected. Objects with many edges can be better coated by electrodeposition than by any other painting technique.

Uniform thickness can be a problem, especially with relatively highly pigmented primers: as the applied coating follows closely the surface contours of the metal, a rough metal will give a rough primer surface.

The paint films are relatively thin, varying from 15 to 30  $\mu\text{m}$ , depending on coating composition and application parameters. The substrate must be conductive and only the first layer can be applied by electrodeposition.

These coatings present very high performances if well applied and require efficient methodology to evaluate their corrosion properties after application and ageing. The corrosion protection of this layer necessitates the development of electrochemical techniques allowing a rapid detection of microdefects, loss of barrier properties, delamination propagation on scratched samples,... This information should ideally be available in a short time, before the defects are observed by visual or optical inspections. In the following paragraph, the electrochemical impedance spectroscopy is described for the evaluation of the main degradation risks of electrocoating during lifetime.

### 3. Electrochemical impedance spectroscopy

This part of the chapter will describe the principle, the interpretation of impedance spectra by using the raw parameters and the electrical equivalent circuits. The evaluation of performances of electrocoatings will be discussed and illustrated by some practical examples.

#### 3.1 Principle

Electrochemical impedance spectroscopy is a non-stationary technique based on the differentiation of the reactive phenomena by their relaxation time. The electrochemical system is submitted to a sinusoidal voltage perturbation of low amplitude and variable frequency. At each frequency the various processes evolve with different rates, enabling to distinguish them.

A weak amplitude sinusoidal perturbation is generally superimposed to the corrosion potential or open circuit potential:

$$\Delta U = |\Delta U| \sin \omega t \quad \text{with } \omega = 2\pi f$$

where  $f$  is the frequency (Hz) of the applied signal.

This perturbation induces a sinusoidal current  $\Delta I$  superimposed to the stationary current  $I$  and having a phase shift  $\varphi$  with respect to the potential:

$$\Delta I = |\Delta I| \sin(\omega t - \varphi)$$

These values can be represented in the complex plane:

$$\Delta U = \Delta U_{re} + i\Delta U_{im}$$

$$\Delta I = \Delta I_{re} + i\Delta I_{im}$$

The complex impedance is defined as:

$$Z = \frac{\Delta U}{\Delta I} = Z_{re} + iZ_{im}$$

The impedance can also be represented by a modulus  $|Z|$  and a phase angle shift  $\varphi$ :

$$|Z| = \sqrt{Z_{re}^2 + Z_{im}^2}$$

$$\text{tg } \varphi = \frac{Z_{im}}{Z_{re}}$$

The impedance data can be represented in two ways:

- Nyquist spectrum:  $-Z_{im}$  as a function of  $Z_{re}$
- Bode spectrum:  $\log |Z|$  and phase angle  $\varphi$  as a function of  $\log f$

The electrochemical measurements are generally carried out using a conventional three-electrode cell filled with the electrolytic solution (Figure 3): a working electrode (the sample



under study), a counter electrode (often a platinum grid or plate) and a reference electrode (such as Ag/AgCl/KCl sat.).

The exposed surface area must be accurately determined and should be high enough when coating capacitance needs to be evaluated.

The impedance measurements are performed over large frequencies ranges, typically from 100 kHz to 10 mHz using amplitude signal voltage in the range of 5 mV to 50 mV rms. The amplitude is strongly depending on the studied system. For an electrocoating system, a classical value of 20 mV rms is chosen to characterize intact coatings. However, for EIS measurements on scratched samples, the response of the exposed metal being dominant, a perturbation of maximum 5 mV rms is used. The EIS spectra can be acquired using the combination of a potentiostat with a frequency response analyser or with a lock-in amplifier.

As the temperature may strongly influence the kinetics of water or oxygen diffusion, the corrosion rates and the mechanical properties of the film, the measurements are preferably carried out at controlled temperature.

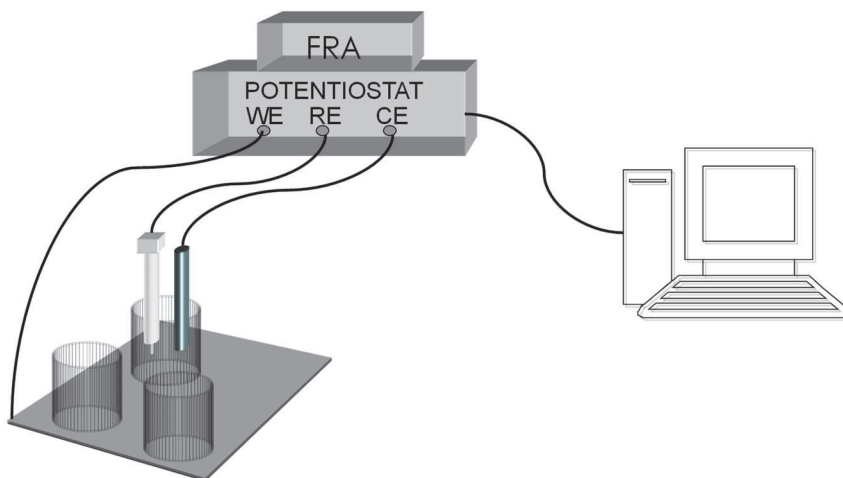


Fig. 3. Schematic representation of the electrochemical cell

### 3.2 Electrical equivalent circuit

The interpretation of impedance data is generally based on the use of electrical equivalent circuits representative of the electrochemical processes occurring at the sample/electrolyte interface. These circuits are built from the appropriate combination of simple electrical elements (capacitors, resistors,...).

An intact coating behaves as a dielectric and can be represented by a capacitor. When in contact with an electrolyte, the coating starts to absorb water and the electrolyte enters the pores of the coating. The electrical equivalent circuit describing this system is represented in Figure 4. While entering the pores, the electrolyte causes a decrease of the pore resistance  $R_p$  which can be considered as initially infinite.

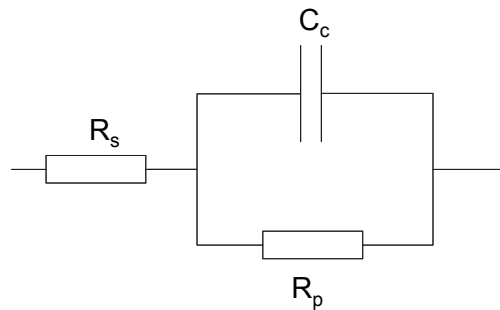


Fig. 4. Electrical equivalent circuit of an intact coating in contact with an electrolyte;  $R_s$  is the electrolyte resistance,  $C_c$  the coating capacitance and  $R_p$  the pore resistance.

Once the corrosion reactions start at the metal/electrolyte interface under the coating or at the base of the pores electrical elements related to the newly created interface have to be included in the equivalent circuit. This is illustrated in Figure 5 in which a circuit describing the exposed metal/electrolyte interface is added to the coating electrical elements. This circuit consists of the double layer capacitance and an electrical element describing the electrochemical reactions at the metal/electrolyte interface.

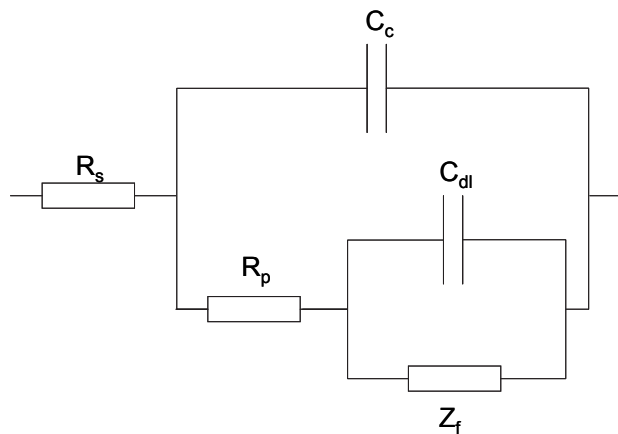


Fig. 5. Electrical equivalent circuit of a coating in contact with an electrolyte (degradation in process).  $R_s$  is the electrolyte resistance,  $C_c$  the coating capacitance,  $R_p$  the pore resistance,  $C_{dl}$  the double layer capacitance,  $Z_f$  an electrical element representing the electrochemical reactions of the metallic substrate in contact with the electrolyte [33].

The fitting of the impedance data to the circuits of Figures 4 or 5 allows obtaining the electrical parameters describing the coating:

- $C_c$ , the coating capacitance defined by

$$C_c = \frac{\epsilon_0 \epsilon_r A}{d}$$

where  $\epsilon_0$  is the vacuum permittivity or the permittivity of the free space,  $\epsilon_r$  is the relative permittivity or coating dielectric constant,  $A$  the coating surface area and  $d$  its thickness.

The dielectric constant of a typical polymeric material is about 3 – 8 and that of water being at 78.5 at 25°C. During water absorption by the coating, its dielectric constant increases with the resulting increase of the coating capacitance ( $A$  and  $d$  considered as constant). It is possible to estimate the amount of absorbed water. The most common model to calculate the volume fraction of absorbed water was developed by Brasher and Kingsbury [34] and is given by:

$$\phi = \frac{\log(C_t/C_0)}{\log(\epsilon_w)}$$

where  $C_t$  is the coating capacitance at time  $t$ ,  $C_0$  the capacitance of the 'dry' coating and  $\epsilon_w$  is the water dielectric constant.

The use of this equation is however restricted to some limitations:

- The increase of the coating capacitance should only be due to water absorption
- Water is uniformly distributed inside the coating
- The water uptake remains low and no swelling occurs
- No interaction between water and the polymer may occur
- $R_p$ , the pore resistance defined as

$$R_p = \frac{\rho d}{A_p}$$

where  $\rho$  is the electrolyte resistivity in the pores,  $d$  the pore length ( $\sim$ coating thickness) and  $A_p$  the total pore surface area.

$R_p$  decreases as the electrolyte penetrates the coating and fills the pores. The decrease of  $R_p$  with time may be related to the increase of  $A_p$  which can be explained by an increase of the number of filled pores or an increase of their area if delamination occurs.

- $C_{dl}$  : the double-layer capacitance which is proportional to the active metallic area  $A_w$  (area in contact with the electrolyte).
- $Z_f$  which in the simple case of a charge transfer-controlled process can be replaced by  $R_{ct}$ , the charge-transfer resistance inversely proportional to the active metallic area.

In practical, the measured impedance spectra may differ from ideal or theoretical behaviour. The loops (or time constants) do not show a perfect semi-circle shape in Nyquist representation. This non-ideal behaviour may arise from coating heterogeneities as roughness, inhomogeneous composition,... In such a case the coating cannot be described by a simple capacitor. This one is generally replaced by a constant phase element (CPE) whose impedance is given by:

$$Z_{CPE} = \frac{1}{Y_0} (i\omega)^{-n}$$

$n$  accounts for non-ideal behaviours: when it equals to 1, the CPE is a pure capacitance and when it equals zero, the CPE is a pure resistance.

Misinterpretation of coating evolution may arise from an erroneous impedance data fitting. Consequently, it is sometimes better to restrict the data interpretation to simple parameters as the global resistance of the system represented by the low frequency impedance modulus ( $|Z|_{0.01\text{Hz}} \sim R_s + R_p + R_{ct}$ ) and the coating capacitance values obtained from high frequency impedance modulus [35].

The coating capacitance can indeed be determined from the impedance modulus at a fixed frequency (10 kHz for example) and can thus be calculated from:

$$C_c = \frac{1}{2\pi 10^4 |Z|_{10\text{kHz}}}$$

### 3.3 Barrier properties

The barrier properties of an electrocoating are maintained during ageing if a capacitive behavior is maintained over the whole frequency range. Due to the high performances of cathaphoretic coatings, the immersion time must be very long before observing changes in the EIS spectra. So some procedures to accelerate the ageing can be used in order to be able to differentiate the behavior of two different systems. Two methods will be discussed in this chapter, the use of salt spray and AC/DC/AC tests.

#### 3.3.1 Immersion test

One example to illustrate the evaluation of the barrier properties is to investigate the EIS response of an experimental epoxy coating cathaphoretically deposited on a 6016 aluminium alloy (typically used in the automotive industry). Two pretreatments are compared: acid etching and a commercial Zr/Ti conversion coating. The evolution of the coating properties is evaluated by EIS after different immersion times in NaCl 0.5 M electrolyte. Systems having different pretreatments are compared in terms of barrier properties, water uptake, and apparition of a second time constant in the EIS spectra. Figures 6a and b show the evolution as a function of time in the NaCl solution of the impedance modulus versus frequency of coated samples (Bode-modulus plots). Different stages can be distinguished: capacitive (C), mixed capacitive and resistive (CR) and resistive (R) behaviours. In the early times of immersion, the coating acts as a barrier against water and electrolyte (stage C). The coating behaves as a dielectric and the resulting impedance modulus logarithm varies linearly as a function of the frequency logarithm. The loss of barrier properties corresponds to the penetration of water and electrolyte through the pores and defects of the coating up to the metal. At this stage (CR), the low-frequency modulus progressively decreases reflecting the decrease of the pore resistance ( $R_p$ ). The time at which the low-frequency modulus starts to decrease varies slightly with the surface preparation prior to coating: an average of 40 days for non pre-treated samples (NP) (Figure 6a) and 50 days for Zr/Ti pre-treated samples (ZT) (Figure 6b). For both surface preparations, a rapid decrease of the low-frequency modulus is observed from the moment the coating lost its barrier properties. Anyway, this experience evidences the importance of the surface pretreatment on the barrier properties of the cathaphoretic electrocoating. This can be explained by a more homogeneous surface on the pretreated substrate showing an uniform electrochemical activity during cathodic electrodeposition. Non pretreated samples are generally rather heterogeneous. Hydrogen evolution reaction may thus vary from one point to another with the consequent risk of appearance of coating micro-defects after coating curing.

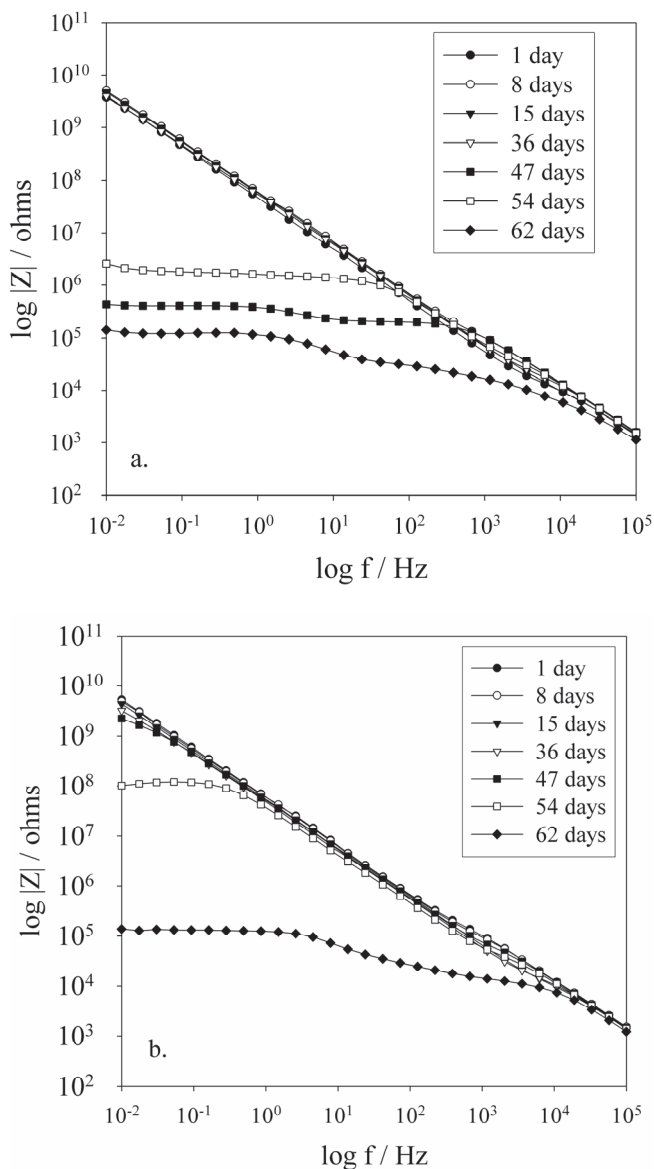


Fig. 6. Bode-modulus plots for different immersion times in NaCl 0.5 M of electrocoated aluminium samples without pre-treatment (a) and with a Zr/Ti pre-treatment (b) [36].

Once the electrolyte reaches the base of the pores, corrosion of the metal may start. Corrosion may significantly affect the adhesion of the coating by the increase of pH accompanying the oxygen reduction or by the presence of corrosion products. The loss of adhesion will cause an increase of the active metal surface area so that a second loop or time

constant ( $R_{ct}$   $C_{dl}$ ) appears in the Bode-diagrams. The second time constant starts to be visible after 47 days and 62 days for NP and ZT samples respectively.

Coated samples were also exposed to salt fog. In that case, the samples were periodically removed from the salt spray chamber and transferred into the electrochemical cell filled with NaCl 0.5M. After an EIS measurement the samples were immediately returned to the salt fog chamber so that the time spent out of the chamber was as short as possible (maximum one hour).

As with the continuous immersion test, the three stages of degradation are also observed with the salt spray test combined with EIS. There is a rather good correlation between the results obtained with both tests. Indeed, the EIS spectra obtained as a function of immersion time or salt fog exposure show that the Zr/Ti pre-treatment enhances the corrosion resistance of the coating. Moreover for ZT samples, after 40 days of exposure to salt fog the total impedance is still high as for the immersion test after the same testing period. The time at which non pre-treated samples lose their barrier properties is somewhat shorter for salt fog exposure than for the immersion test. This difference can be accounted for by the higher exposure temperature and the higher oxygen concentration due to continuous aeration in the case of salt fog exposure. At the end of both tests, no visible signs of deterioration were detected while significant changes in the EIS response occurred.

The pore resistance was determined by fitting the impedance diagrams with the electrical equivalent circuit model of Figure 5. In agreement with the observed decrease of the low-frequency impedance modulus,  $R_p$  shows an important decrease as a function of exposure (Figure 7), especially for samples NP which give  $R_p$  values below  $10^7$  ohms  $cm^2$  after 40 days of exposure. The pore resistance is higher for ZT samples than for NP samples suggesting that the pre-treatment could also have a beneficial role on the barrier properties of the coating.

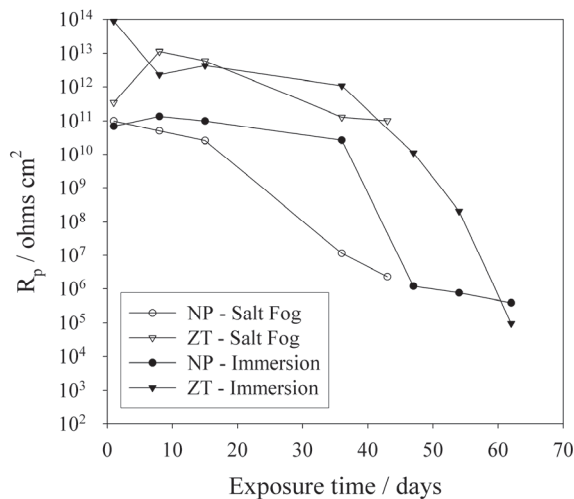


Fig. 7. Pore resistance as a function of exposure time to salt fog or to an immersion test for NP and ZT samples [36].

The coating capacitance values reflect water and electrolyte ingress in the coating. The  $C_c$  values are almost constant versus exposure time for samples NP and ZT exposed to both tests, meaning that during the period from 1 to 60 days there is probably no significant water absorption by the coating. Cathodically deposited coatings are known to be rather impermeable to water so that there is only a slight absorption of water by the coating at the early moments of contact as illustrated in Figure 8. The volume fraction of water absorbed by the coating can be estimated from Brasher and Kingsbury and is about 0.8% which is very low.

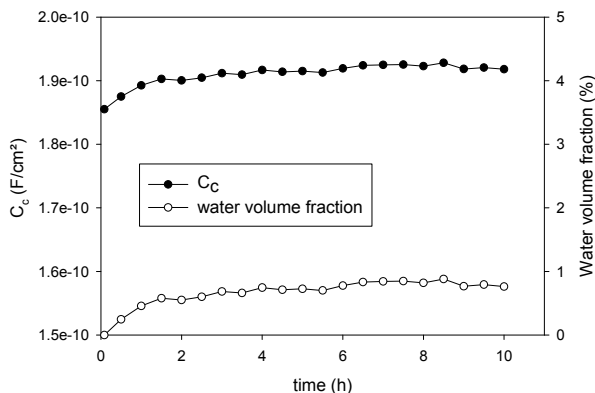


Fig. 8. Coating capacitance as a function of exposure time in NaCl 0.5M for a ZT sample.

### 3.3.2 AC/DC/AC cycles

The ac/dc/ac procedure was developed in order to assess the anti-corrosive properties of a coating in a very short time [37-41]. This procedure consists of a combination of cathodic polarization (dc) and EIS measurements (ac). After a first ac measurement at the open-circuit potential, the sample is treated for a short time by a constant cathodic potential (dc). Typically, during the dc period, the tested sample is cathodically polarized at  $-3V/ref$  during 2 h followed by a 3 h relaxation time until it recovers a new steady state. These steps are repeated by means of programmed cycles until the loss of the coating protective properties is observed in the ac spectrum. The evolution of the impedance spectrum is generally attributed to both coating degradation due to the decrease of pore resistance and to delamination process, which is accelerated by  $OH^-$  production at the metal surface during cathodic polarization.

As the density of pores or micro-defects reaching the metallic substrate decreases with the coating thickness, using thinner coatings may give rise to even more pronounced degradation and provide useful information in shorter time. In the following example the ac/dc/ac procedure was performed with two different electrocoatings (A and B) differing by their content in plasticizer. These coatings were applied with different thicknesses (14, 17 and 20  $\mu m$ ) by changing the electrodeposition time and maintaining the application voltage constant. An example of the resulting impedance spectra is presented in Figure 9 for a Zr/Ti pretreated sample with coating A applied with 14  $\mu m$  thickness.

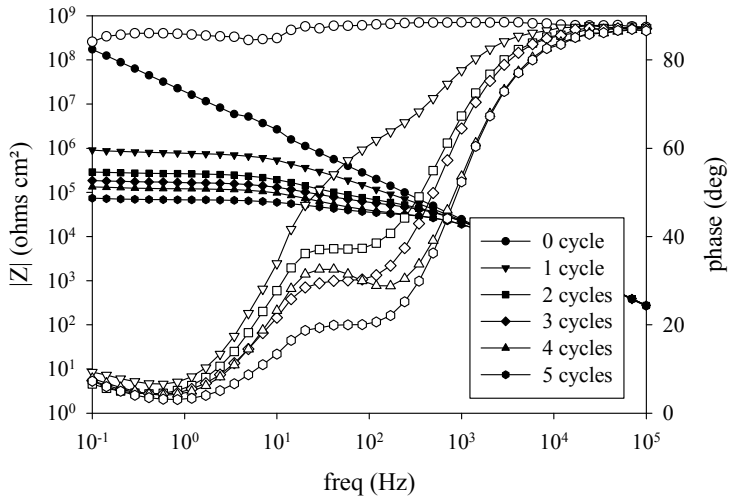


Fig. 9. Bode (modulus and phase) plots for an electrocoated sample (coating A) undergoing ac/dc (-3V/ref)/ac cycles. Electrolyte : NaCl 0.5M, exposed surface area : 4.9 cm<sup>2</sup>.

Though the initial barrier properties are high and the behavior purely capacitive, the total impedance of the system strongly decreases after one cycle. Afterwards the barrier properties continue to decrease gradually with the number of cycles. With low thickness, the decrease of  $R_p$  is even more pronounced. The faster decrease of the barrier properties when the coating thickness is reduced is probably due to a higher density of pores reaching the metallic substrate.

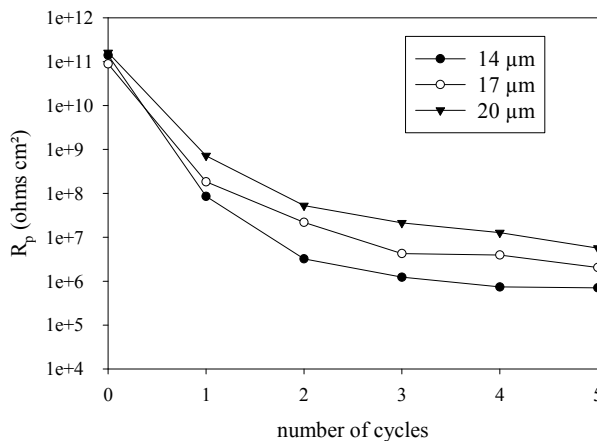


Fig. 10. Pore resistance as a function of the number of ac/dc cycles for coating A with a Zr/Ti pretreatment.



The presence of a distinguishable second time constant from the first ac/dc cycle allows the determination of the electrical parameters related to the metal/electrolyte interface. These parameters were obtained by fitting the impedance spectra with the equivalent circuit of Figure 5 for the different coating thicknesses. An increased electrochemical activity at the metal/electrolyte interface results from the application of ac/dc/ac cycles. As a consequence the double layer capacitance ( $C_{dl}$ ) shows a rather important increase with the number of cycles (Figure 11).

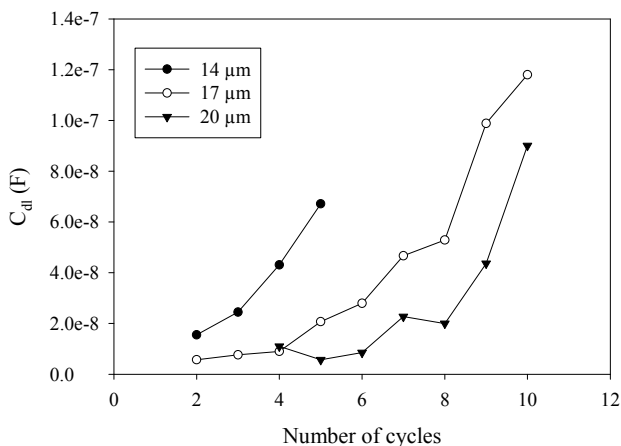


Fig. 11. Double layer capacitance as a function of the number of cycles as determined from fitting the impedance spectra with the electrical equivalent circuit from Figure 5. Electrocoating A applied with different coating thicknesses on etched aluminium samples (without pretreatment).

Applying a cathodic polarization induces a fast penetration of the electrolyte through the total thickness of the coating. Delamination occurs in the pore regions and favors the blisters formation. The increase of the double layer capacitance is less pronounced and appears later when the coating thickness is higher as illustrated in Figure 11. For a same number of cycles, the double layer capacitance is indeed higher for a lower coating thickness. This can be accounted for by the higher density of pores reaching the metal leading to a total higher value of the active metallic surface area. Smaller thicknesses consequently result in a rapid start of the corrosion process and in a consequent adhesion loss of the coating from the substrate.

Applying an appropriate pretreatment as Zr/Ti leads to higher barrier properties and to a better resistance to cathodic delamination as accounted for by the smaller double layer capacitance values determined with ZT samples whatever the electrocoating applied (Figure 12). A comparison between two coatings (A and B) differing by their content in plasticizing agent is also possible on the basis of the AC/DC cycles as illustrated in Figure 12. The coating with the higher content in plasticizer shows lower barrier properties and a high sensitivity to cathodic delamination accounted for by the important increase of  $C_{dl}$  with the number of cycles especially on NP samples. The addition of plasticizing agent leads to better

rheological properties during curing but is also responsible of a less curing density and thus to higher porosity and water permeability. The barrier properties of such coatings may however be enhanced through an appropriate adaptation of the coating parameters (such as voltage for example). AC/DC cycles thus offer a rapid method to discriminate “bad” coatings and to optimize the application parameters.

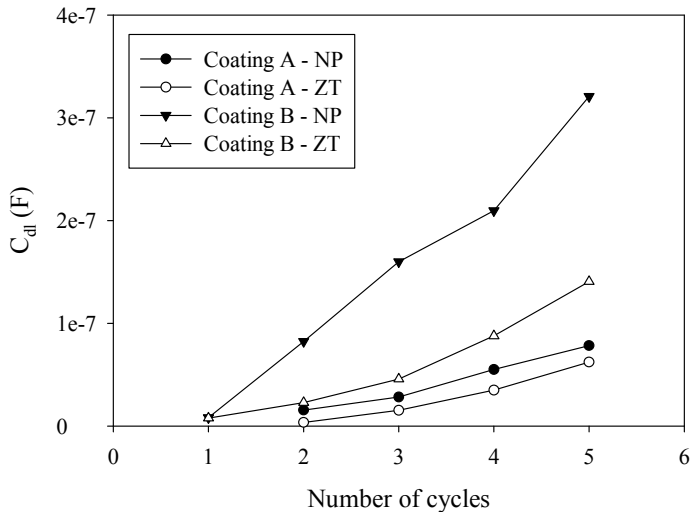


Fig. 12. Double layer capacitance as a function of the number of cycles as determined from fitting the impedance spectra with the electrical equivalent circuit from Figure 5. Electrocoating A and B applied on etched aluminium samples (NP) and on Zr/Ti pretreated samples (ZT). Coating thickness: 14  $\mu\text{m}$ .

### 3.4 Evaluation of delaminated area from a defect

The most common way to evaluate the delamination of a coating is to scratch the coating, reaching the metallic substrate, to expose the samples to an accelerated ageing test and to evaluate after a determined exposure time the total delaminated area from the scratch. It is however also possible to follow the evolution of the delamination process with EIS measurements on scratched samples [21, 22, 42-45]. In that case, the evaluation of the delaminated area is based on the determination of the wet area where the corrosion reactions take place. Nevertheless, in order to obtain quantitative values of this surface by EIS spectra the corrosion products coming from the corrosion phenomenon must be dissolved before EIS determination. The apparition of these corrosion products may also be avoided by cathodic polarization. In each case the operating parameters must be well controlled to avoid a subsequent degradation or induce a degradation process not representative of a natural ageing. These parameters were investigated to identify a new electrochemical tool to evaluate the improvement of the interface stability of metal/electrocoating in order to identify the sensitivity to filiform corrosion of electrocoated aluminium alloys, the electrocoating coverage of steel edges and the delaminated area during a salt spray test.

Aluminium alloys are known to be particularly susceptible to filiform corrosion which is a specific delamination which occurs under atmospheric conditions with high relative humidity (50-90%). This specific type of delamination is an anodic undermining driven by a differential aeration cell created between the head front of filament (anode) and the defect (cathode). This corrosion phenomenon can be revealed by EIS on scratched samples [21, 22, 44]. In the following example, the electrocoated aluminium alloy samples were scratched with a cutter reaching the metallic substrate. The linear defect produced was  $2 \pm 0.02$  cm long and  $40 \mu\text{m}$  width with an area of about  $0.8 \text{ mm}^2$ . The width and area of the defect were controlled with the help of an optical microscope. The procedure used to initiate (1 hour in the HCl vapours) and propagate filiform corrosion was the same as that adopted in the ISO/DIS 4623 standard with a shorter exposure time in the humid chamber. The climatic conditions during exposure were  $82 \pm 3\%$  relative humidity and  $40^\circ\text{C} \pm 2^\circ\text{C}$ . The samples were then analysed by EIS at room temperature in  $0.1 \text{ M Na}_2\text{SO}_4$  acidified at pH ranging from 1 to 3 by adding sulphuric acid. Different immersion times in the electrolyte solution were explored. The analysis of the EIS data is based on the fitting of the spectra with the electrical equivalent model of Figure 5. However in the presence of a macroscopic defect as that obtained with a scratch, the time constant associated with the coating is generally shifted towards higher frequencies than those conventionally explored. The low/mid frequency time constant accounts for the electrochemical processes occurring at the exposed metallic substrate.  $C_{dl}$  and  $R_{ct}$  are two parameters used to specify the delamination or filiform corrosion of the coating. The choice of an acidified electrolyte solution ( $0.1 \text{ M Na}_2\text{SO}_4$  at pH = 2) allows to dissolve the corrosion products formed under the coating during exposure to the humidity chamber. The immersion time in the electrolyte is also an important parameter. Actually, the immersion time has to be long enough to dissolve the corrosion products formed during the test. However, too high immersion times may be accompanied by the growth of new corrosion products due to the reaction of the metal with the testing electrolyte. Figure 13 illustrates the effect of immersion time in the testing electrolyte (sodium sulphate at pH 2) for an electrocoating applied on etched aluminium (without pretreatment) and exposed 48h to the standard filiform corrosion test (82% RH and a temperature of  $40^\circ\text{C}$ ). After immersion for 1 h in the testing electrolyte, two time constants can be distinguished in Bode-phase diagram. The time constant observed at high frequency can be assigned to the presence of corrosion products as discussed in ref 46-48. This means that the corrosion products formed under the coating during exposure to humidity are not completely dissolved before EIS measurement. The low frequency time constant attributed to the corrosion process is displaced to lower frequencies indicating a slowdown of the process which can be explained by the contribution of diffusion in the electrochemical process occurring at the metal/electrolyte interface [49]. Longer immersion times in the electrolyte allow the dissolution of the corrosion products present in the defect as only one time constant is detected from 8h of contact with the electrolyte.

In order to enhance the dissolution of the corrosion products in a shorter time, measurements were also carried out at pH = 1. The impedance data in the Bode phase representation obtained after 48 h in the climatic chamber, 4 h in the test solution at pH = 1 are shown in Figure 14. To get a better understanding of the influence of pH, measurements were also made at pH = 3. By acidifying the electrolyte solution, the corrosion products are dissolved within shorter immersion times and thus, the time constant due to corrosion products in the impedance data disappears. On the contrary, after 4 h of immersion in the electrolyte solution at pH = 3, the time constant associated with the electrochemical reaction

can be explained by a higher contribution of diffusion process than at  $\text{pH} = 2$ . At  $\text{pH}=1$ , the observed time constant is only related to the electrochemical reaction at the metal/electrolyte interface in the scratch and inside the filaments.

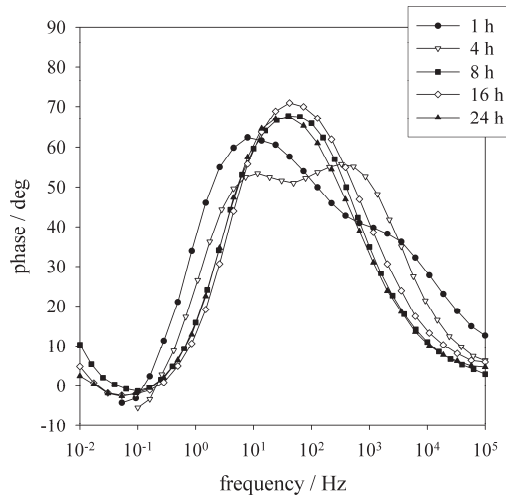


Fig. 13. Bode-phase diagrams for different immersion times in the sulphate electrolyte solution at  $\text{pH} 2$ . Data obtained with aluminium samples etched and electrocoated without any pre-treatment; exposure time in the humidity chamber: 48 h [48].

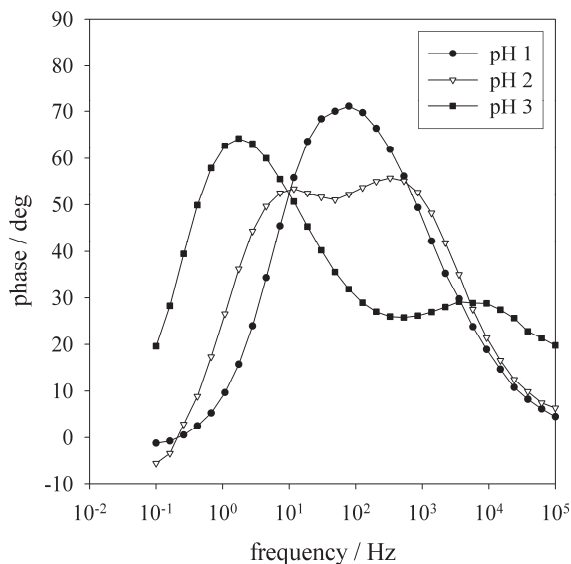


Fig. 14. Bode-phase diagrams at different  $\text{pH}$  of the sulphate electrolyte solution. Aluminium samples coated without pre-treatment; data obtained after 48 h of exposure to humidity chamber and 4 h of immersion in the electrolyte solution [48].

This simple procedure which was initially developed to the study of filiform corrosion on coated aluminium may also be used to evaluate the delaminated area of scratched samples exposed to any type of accelerated ageing test. In the following example, EIS was performed on electrocoated aluminium 6016 samples exposed for maximum 10 days to a neutral salt fog. After exposure, the scratched samples were assembled in a three-electrode electrochemical cell filled with  $\text{Na}_2\text{SO}_4$  0.1 M at pH 1. The impedance measurements were carried out after 1 h, time necessary to reach stationary conditions (stable corrosion potential). The resulting impedance spectra only show one time constant corresponding to the second time constant of electrochemical circuit shown in Figure 5.

$C_{dl}$  values were determined by fitting the impedance spectra with one time constant electrical model describing the electrochemical reactions occurring at the exposed metal surface. The  $C_{dl}$  values were then divided by the double layer capacitance of the bare metal to give the evolution of the active metal area as a function of exposure (Figure 15). Higher

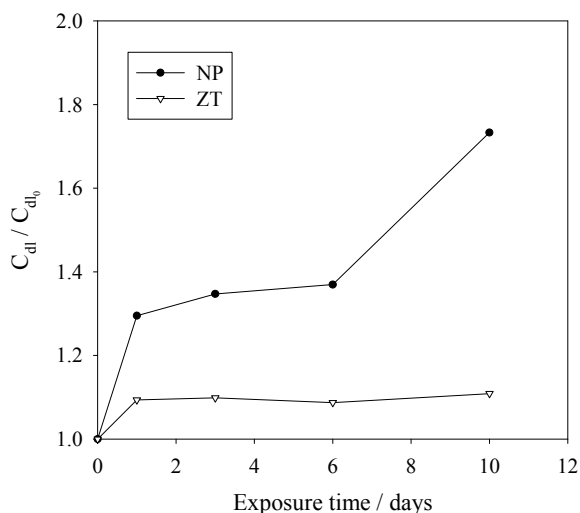


Fig. 15. Values of the double layer capacitance  $C_{dl}$  divided by the bare metal double layer capacitance  $C_{dl0}$  as a function of exposure to salt fog of scratched NP and ZT samples [36].

double layer capacitance values are observed for NP samples explained by the poor adhesion of the coating when the samples are not pre-treated before being painted. Moreover non pre-treated samples show a significant increase of the double layer capacitance as a function of the exposure time to salt fog and thus an increase of the delaminated area. For the Zr/Ti pre-treated samples, the values are constant during the first 10 days of exposure to salt spray. Accordingly, the tendency observed for  $C_{dl}$  values of both samples fully agrees with the visual observation of a development of filiform corrosion on non-pre-treated samples while Zr/Ti pre-treated samples were not degraded after 10 days of salt fog exposure. After this period, the solubilization of the corrosion products formed on non-pre-treated samples becomes harder. As a consequence, a rather accurate estimation of the extent of filiform corrosion or delamination can be only obtained for short exposure times. However in the present case 10 days of exposure is long enough to distinguish the

behavior of the two types of samples (NP and ZT) and to observe the increase of the delaminated area on non pre-treated samples. Consequently, combining exposure to salt fog of intact and scratched samples and following their degradation by EIS allow the evaluation of the influence of the pre-treatment on the loss of barrier properties and on the coating adhesion to the substrate.

### 3.4.1 Edge corrosion

In spite of the ability of cathodic electrocoating to cover the totality of the car body the electrocoat paints are sensitive to edge corrosion [50]. The edge corrosion generally results from the absence of film or low film build at the edges responsible of a premature corrosion. The edge coverage is especially linked to the flow properties of the coating during the baking process. High-edge coverage coatings are developed by adding rheological agents to the coating formulation [51-53]. The edge coverage can also be improved by modifying the electrocoat application parameters as the voltage, thickness or by the addition of a resistance in the circuit [50]. At present, to characterize the protection offered by cataphoretic coatings against edge corrosion, use is made of knife blades of which edge has a known angle of 38°. After a close examination of the knife blades, these are coated and then undergone a 7 days neutral salt fog exposure (35°C, 5% NaCl) (NF X 41-002). After exposure the blades are rinsed with deionized water and dried. The corrosion is then characterized by numbering the rust spots that appeared on the edges. Though this quotation is generally made with the help of a microscope it is not easy to count every single rust spot [50, 54]. This method is thus highly time consuming, laborious and rather subjective since the results may depend on the operator. Different samples could be used instead of the knife blades as for example ultra-thin or perforated panels or the Volvo grooved steel cylinder. Such samples could improve the visual detection or differentiation of edge corrosion but would not accelerate the test.

Electrochemical methods could be used to characterize the edge-corrosion protection of electrocoated knife blades and to get a short time evaluation of the parameters of the coating deposited on the blade edge.

In the following example, knife blades covered with a 20  $\mu\text{m}$  coating thickness (thickness measured on the flat part of the blade) were exposed to salt fog for 7 days. The number of rust spots observed by microscope is given in Figure 16. These values present a rather important dispersion which can be attributed to the difficult numbering of rust spots, especially when the coating is highly degraded. Despite this dispersion, it is clear that the coating containing 3.5% of rheological agent is less corroded than the one containing 1%. Thus, a slight increase in rheological agent content probably leads to a better edge coverage and a subsequent higher resistance to edge corrosion. The influence of the coating thickness was studied for the coating containing 1% of rheological agent. Knife blades covered with 5, 10 and 20  $\mu\text{m}$  coating thickness (measured on the flat part) were exposed to salt fog for 7 days. As shown in Figure 16 increasing the coating thickness improves the resistance to edge corrosion since for a 20  $\mu\text{m}$  thickness no rust spot was detected. However it is not possible to differentiate the 5 and 10  $\mu\text{m}$  thicknesses on the basis of the salt fog exposure since the average number of rust spots are very close for these thicknesses.

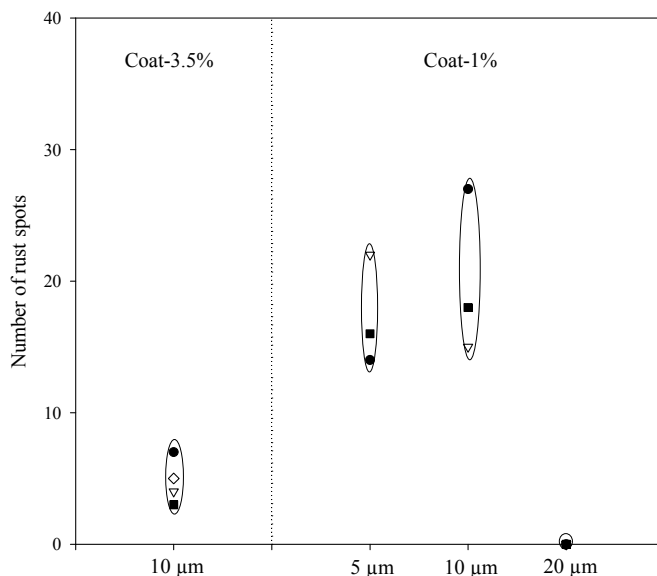


Fig. 16. Number of rust spots after 7 days of salt fog exposure

Different electrochemical methods can be used to characterize the blade edge/electrolyte interface. The idea is to find a test which could provide a rapid evaluation of the total exposed metallic area at the base of the pores or defects on the blade edge. Impedance measurements can provide this information. However, fitting the impedance spectra with the electrical equivalent circuit for an organic coating is not always possible. Another manner to obtain the exposed metallic area is to polarize the sample at a sufficient cathodic potential causing cathodic reaction as hydrogen evolution. The measured current will be proportional to the total exposed metallic area without being affected by the presence of corrosion products. To illustrate this, cathodic polarization measurements were performed on coated knife blades. The current measured at  $-3V/Ag/AgCl/KCl(sat)$  is used to distinguish different coated systems. In the present case the influence of the coating thickness of a coating containing 1% of rheological modifier is investigated. As illustrated in Figure 17, the current density at  $-3V/Ag/AgCl$  shows an important decrease with coating thickness. The lowest current density was measured for a coating thickness of  $20\ \mu m$  for which the exposed metal area is thus the smallest in agreement with the smallest number of rust spots observed after salt fog exposure. Moreover there is a noticeable difference in the current densities between 5 and  $10\ \mu m$  coating thicknesses, for which no distinction was possible on the basis of the salt fog exposure test. The results obtained by electrochemical measurements thus show a good correlation with the salt fog exposure test. However the time necessary to obtain the same information is very short since a cathodic polarization measurement takes about half an hour while the salt fog test necessitates 7 days of exposure.

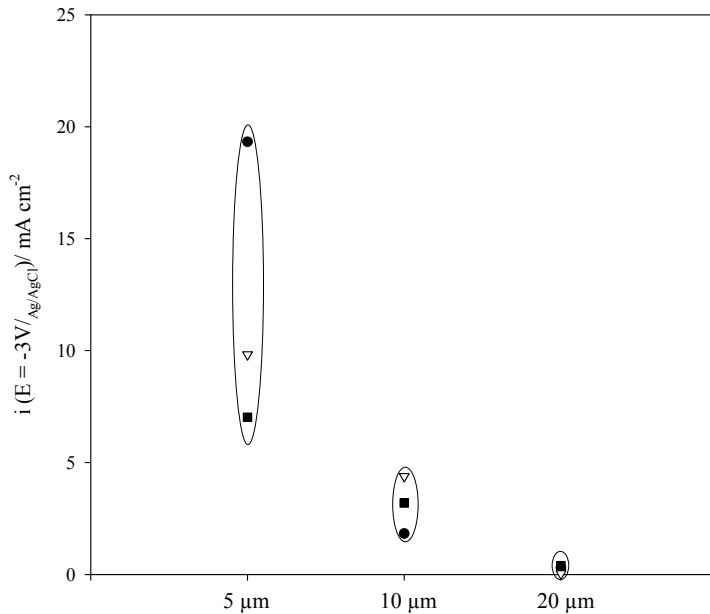


Fig. 17. Current density at a cathodic potential of  $-3V_{Ag/AgCl}$  for different coat-1% thicknesses (measured on the flat part) deposited on knife blades.

#### 4. Conclusions

Cataphoretic electrodeposition is an industrial process which allows obtaining high coating performances responding to high quality requirements of automotive industry. Moreover as it is water-based and formulated without lead and limited VOC content this coating system has a low impact on the environment.

The important challenges in development of new coatings is to assure the adhesion and barrier properties with new environmentally friendly pre-treatments, to be applicable whatever the nature of the substrate, to cover all the car body parts even the recessed areas and the edges and to be scratch resistant. As showed by some examples, Electrochemical Impedance Spectroscopy is a powerful tool to evaluate in short times the behaviour of intact and scratched electrocoated samples. The EIS procedures can give more quantitative information compared to the classical ageing tests. However this technique needs an accurate control of the operating conditions. Furthermore the interpretation of the results needs an appropriate choice of the electrical equivalent circuits to describe the system under study.

#### 5. Acknowledgments

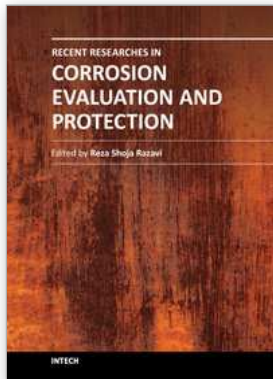
This study was performed in the framework of the Opti2Mat project financially supported by the Walloon region in Belgium.



## 6. References

- [1] Beck, Fundamentals of Electrodeposition of Paint, BASF, 1979, pp. 1-55
- [2] T. Brock, M. Groteklaes, P. Mischke, *European Coatings Handbook*, Verlag, Hannover, 2000, pp. 279-285
- [3] E. Almeida, I. Alves, C. Brites, L. Fedrizzi; *Prog. Org. Coat.* 46 (2003) 20
- [4] K. Arlt, *Electrochim. Acta* 39 (1994) 1189
- [5] L. Krylova, *Prog. Org. Coat.* 42 (2001) 119
- [6] C.M Reddy, R.S Gaston, C.M Weikart, H.K Yasuda; *Prog. Org. Coat.* 33 (1998) 225
- [7] C. A. Ferreira, S. Aeiyaach, A. Coulaud, P. C. Lacaze; *J. Appl. Electrochem.* 29 (1999) 259
- [8] M. Fedel, M.-E. Druart, M. Olivier, M. Poelman, F. Deflorian, S. Rossi; *Prog. Org. Coat.* 69 (2010) 118
- [9] C.Wu, J. Zhang, *J. Coat. Technol. Res.* 7 (2010) 727
- [10] G. P. Bierwagen, L He, J Li, L Ellingson, D.E Tallman; *Prog. Org. Coat.* 39 (2000) 67
- [11] G.P. Bierwagen, "The Science of Durability of Organic Coatings – A Foreword." *Prog. Org. Coat.*, 15 (1987) 179-185
- [12] F.X. Perrin, C. Merlatti, E. Aragon, A. Margaiilan; *Prog. Org. Coat.* 64 (2009) 466
- [13] N. LeBozec, D. Thierry; *Materials and Corrosion* 61 (2010) 845
- [14] A. W. Hassel, S. Bonk, S. Tsuru, M. Stratmann; *Materials and Corrosion* 59 (2008) 175
- [15] L. Beaunier, I. Epelboin, J.C. Lestrade and H. Takenouti *Surf. Technol.*, 4 (1976) 237
- [16] M.W. Kendig and H. Leidheiser.; *J. Electrochem. Soc.* 23 (1976) 982
- [17] J.D. Scantlebury and K.N. Ho. *JOCCA*, 62 (1979) 89
- [18] T. Szauer. *Prog. Org. Coat.* 10 (1982), 157
- [19] F. Mansfeld, M.W. Kendig and S. Tsai. *Corrosion* 38 (1982) 478
- [20] A. Amirudin, D. Thierry, *Prog. Org. Coat.* 26 (1995) 1
- [21] F. Deflorian, L. Fedrizzi, *J. Adhesion Sci. Technol.* 13 (1999) 629
- [22] D. Loveday, P. Peterson, B. Rodgers; *J. Coat. Tech.* 10 (2004) 88
- [23] D. Loveday, P. Peterson, B. Rodgers; *J. Coat. Tech.* 2 (2005) 22
- [24] F. Deflorian, S. Rossi; *Electrochim. Acta* 51 (2006) 1736
- [25] K. Allahar, Q. Su, G.P. Bierwagen; *Prog. Org. Coat.* 67 (2010) 180
- [26] S. Touzain ; *Electrochim. Acta* 55 (2010) 6190
- [27] T. Breugelmans , E. Tourwé, J.-B. Jorcin, A. Alvarez-Pampliega, B. Geboes, H. Terryn, A. Hubin ; *Prog. Org. Coat.* 69 (2010) 215
- [28] E.C. Bossert et al., U.S. patent 5,880,178 (1999)
- [29] E.C. Bossert et al., U.S. patent 6,042,893 (2000)
- [30] Z. W. Wicks, F.N. Jones, S. P. Pappas, D.A. Wicks, *Organic Coatings Science and Technology*, Third edition, John Wiley & Sons, (2007) 535
- [31] F. Mansfeld, *Electrochim. Acta* 38 (1993) 1891
- [32] D.M. Brasher, A.H. Kingsbury, *J. Appl. Chem.* 4 (1954) 62
- [33] G.P. Bierwagen, D. Tallman, J. Li, L. He, C. Jeffcoate, *Prog. Org. Coat.* 46 (2003) 148
- [34] M. Poelman, M.-G. Olivier, N. Gayarre, J.-P. Petitjean, *Prog. Org. Coat.* 54 (2005) 55
- [35] M. Bethencourt, F.J. Botana, M.J. Cano, R.M. Osuna, M. Marcos *Prog. Org. Coat.* 49 (2004) 275-281
- [36] S.J. Garcia, J. Suay *Prog. Org. Coat.* 59 (2007) 251-258
- [37] M.T. Rodríguez, J.J. Gracenea, S.J. García, J.J. Saura, J. Suay *Prog. Org. Coat.* 50 (2004) 123-131
- [38] S.J. García, J. Suay; *Progr. Org. Coat.* 66 (2009) 306-313

- [39] K.N. Allahar, G. Bierwagen, V.J. Gelling ; *Corr. Sci.* 52 (2010) 1106-1114
- [40] S. Gonzalez, M.A. Gil, J.O. Hernandez, V. Fox, R.M. Souto, *Prog. Org. Coat.* 41 (2001) 167
- [41] J.M.I. McIntyre, H.Q. Pham, *Prog. Org. Coat.* 27 (1996) 201
- [42] F. Deflorian, L. Fedrizzi, S. Rossi, P.L. Bonora, *Electrochim. Acta* 44 (1999) 4243
- [43] M.L. Zheludkevicha, K.A. Yasakau, A.C. Bastos, O.V. Karavai, M.G.S. Ferreira; *Electrochem. Comm.* 9 (2007) 2622
- [44] L. Fedrizzi, F. Deflorian, S. Rossi, *Benelux Metall.* 37 (1997) 243
- [45] L. Fedrizzi, F. Deflorian, S. Rossi, P.L. Bonora, *Mater. Sci. Forum* 289-292 (1998) 485
- [46] M.-G. Olivier, M. Poelman, M. Demuyne, J.-P. Petitjean, *Prog. Org. Coat.* 52 (2005) 263-270
- [47] C.G. Oliveira, M.G.S. Ferreira, *Corr. Sci.* 45 (2003) 139
- [48] N. Blandin, W. Brunat, R. Neuhaus, E. Sibille, *Proc. Eurocorr*, 2004
- [49] Y.-B. Kim, H.-K. Kim, J.-W. Hong *Surf. Coat. Technol.*, 153 (2002) 284-289
- [50] V.C. Corrigan, S.R. Zawacky, PPG Industries, Inc., "Cationic Microgels and Their Use in Electrodeposition", U. S. Patent 5,096,556, 1992
- [51] D. Saatweber, B. Vogt-Birnbrich, *Prog. Org. Coat.* 28 (1996) 33-41
- [52] M. Poelman, M.-G. Olivier, N. Cornil, N. Blandin, *Proc. Eurocorr*, 2006



## **Recent Researches in Corrosion Evaluation and Protection**

Edited by Prof. Reza Shoja Razavi

ISBN 978-953-307-920-2

Hard cover, 152 pages

**Publisher** InTech

**Published online** 25, January, 2012

**Published in print edition** January, 2012

The purpose of this book is to present and discuss the recent methods in corrosion evaluation and protection. The book contains six chapters. The aim of Chapter 1 is to demonstrate that Electrochemical Impedance Spectroscopy can be a very useful tool to provide a complete evaluation of the corrosion protection properties of electro-coatings. Chapter 2 presents results of studies of materials degradation from experimental electrochemical tests and theoretical calculations. Chapter 3 deals with the presentation of the corrosion and corrosion prevention of the aluminum alloys by organic coatings and inhibitors. Chapter 4 addresses the new method of pigment preparation that can improve protection efficiency. The effectiveness of plasma deposited films on the improvement of carbon steel corrosion resistance is discussed in Chapter 5. Chapter 6 deals with the conjugation of carbon nanotubes with organic-inorganic hybrid to prepare hybrid coatings that combine high anti-corrosion efficiency with elevated mechanical resistance.

### **How to reference**

In order to correctly reference this scholarly work, feel free to copy and paste the following:

Marie-Georges Olivier and Mireille Poelman (2012). Use of Electrochemical Impedance Spectroscopy (EIS) for the Evaluation of Electrocoatings Performances, Recent Researches in Corrosion Evaluation and Protection, Prof. Reza Shoja Razavi (Ed.), ISBN: 978-953-307-920-2, InTech, Available from:  
<http://www.intechopen.com/books/recent-researches-in-corrosion-evaluation-and-protection/use-of-electrochemical-impedance-spectroscopy-eis-for-the-evaluation-of-electrocoatings-performances>

# **INTECH**

open science | open minds

### **InTech Europe**

University Campus STeP Ri  
Slavka Krautzeka 83/A  
51000 Rijeka, Croatia  
Phone: +385 (51) 770 447  
Fax: +385 (51) 686 166  
[www.intechopen.com](http://www.intechopen.com)

### **InTech China**

Unit 405, Office Block, Hotel Equatorial Shanghai  
No.65, Yan An Road (West), Shanghai, 200040, China  
中国上海市延安西路65号上海国际贵都大饭店办公楼405单元  
Phone: +86-21-62489820  
Fax: +86-21-62489821

© 2012 The Author(s). Licensee IntechOpen. This is an open access article distributed under the terms of the [Creative Commons Attribution 3.0 License](#), which permits unrestricted use, distribution, and reproduction in any medium, provided the original work is properly cited.